DEVELOPMENT OF A CRYOCATCHER PROTOTYPE FOR SIS100*

L. Bozyk and D.H.H.Hoffmann, TU-Darmstadt and GSI Darmstadt, Germany

P. Spiller and H. Kollmus, GSI Darmstadt, Germany

Abstract

The main synchrotron SIS100 of the FAIR-facility will be operated with high-intensity intermediate charge state heavy ion beams. In order to assure reliable operation with intermediate charge states, a special synchrotron design, including a catcher system for ionized beam ions had to be developed. Intermediate charge state heavy ions suffer from high cross sections for ionization. Due to the dedicated synchrotron layout, ions which have been further stripped by collisions with residual gas atoms are caught by the ion catcher system in the cryogenic arcs. The construction and test of a cryocatcher prototype at GSI is a workpackage of the EU-FP7 project COLMAT. A prototype catcher including cryostat will be set-up at GSI to perform measurements with heavy ion beams of the heavy ion synchrotron SIS18.

ION CATCHER SYSTEM IN SIS100

The ion optical lattice of SIS100 has been designed for the application of a dedicated ion catcher system. By means of this ion catcher system, stripped beam ions are not lost uncontrolled on the beam pipe, but at defined highly localized positions in the cryogenic arcs (see figure 1 and [1]). The loss distribution shown in figure 1, generated by the so called charge separator lattice, allows the installation of an efficient ion catcher system with a dedicated low desorption yield surface. Almost 100% of U^{28+}-ions which loose one more electron can be caught by such a catcher system (see figure 2). The relative charge change due to ionization $q/q\prime$ is the relevant parameter for different deflection angles, the ionization loss distributions, and catching efficiencies. This parameter does not depend on the beam energy. However, the catching efficiency improves with shrinking emittance during acceleration. Since the ionization cross sections decrease for lighter ions, lower catching efficiencies and stronger vacuum dynamics are not an issue. For lower relative charge changes the storage efficiency, the probability for charge exchanged ions to be stored at least for one complete revolution in the ring, emerges.

Figure 3 shows the working principle of the ion catcher system: Ions with changed charge state are separated from the circulating beam in dispersive elements (dipoles). Due to the displacement from the design orbit and the defocusing of the first quadrupole, these ions hit the ion catcher situated in the middle of the quadrupole doublet.
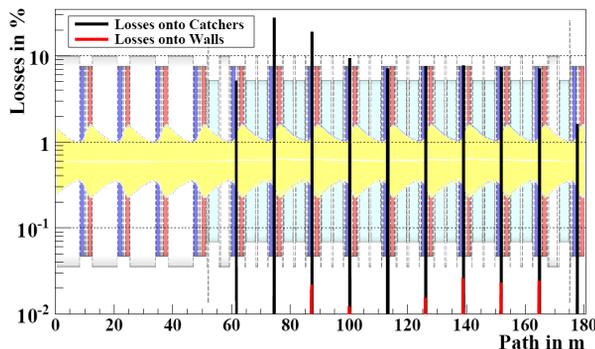
Figure 1: Loss distribution for U^{28+}-ions after losing one electron. Stripped beam ions are lost at highly localized positions in the cryogenic arcs, where the ion catcher will be installed.
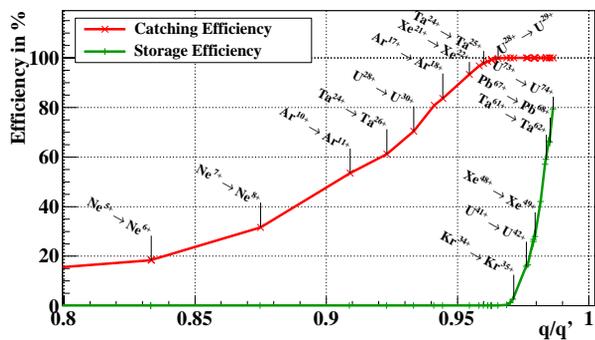
Figure 2: Catching efficiency of the SIS100 ion catcher system. For low relative charge changes, e.g. $U^{28+} \rightarrow U^{29+}$, almost 100% of the lost ions are caught. The storage efficiency is the probabilty for a charge exchanged ion to perform a complete turn before becomming lost.

In SIS18, an ion catcher system [2] was installed successfully, stabilizing the operation with high intensity U^{28+}-beams and shifting the maximum achievable intensity to higher number of particles. In SIS18 the ion current on the ion catcher is measured, which is also foreseen for SIS100. The catcher current indicates ionization losses and scales with the strength of the residual gas pressure dynamics and pressure bumps. Although the ion optical lattice of SIS18 was not optimized for an ion catcher system, the triplet structure provides a catching efficiency of 65%. The recently comissioned current measurements on the catcher system are used to study ionization and capture loss processes.

Due to the lower ionization cross sections, different to the existing SIS18, in SIS100 only on the inner side of the ring ion catchers will be installed. The cross sections for

04 Hadron Accelerators

T19 Collimation and Targetry
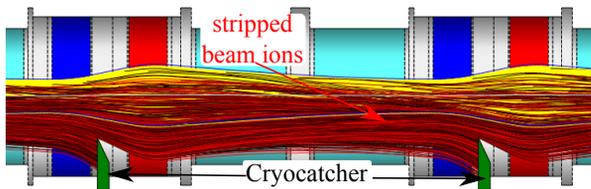
Figure 3: Working principle of the ion catcher system: Ions with changed charge states (red lines) are separated from the circulating beam (yellow) in dispersive elements (dipoles, cyan). Due to the displacement from the design orbit and the defocusing of the first quadrupole (blue) the ions are lost on the ion catcher.

Figure 4: Illustration of the design of the cryocatcher (green): Vacuum chamber in blue, surrounding copper coating in brown, revolving beam in yellow, ionized beam ion trajectories in red, desorbed gases as colored balls, cold surfaces (secondary chamber plates) in brown.

electron capture are only relevant up to the injection energy of SIS18. Already during the acceleration in SIS18 the cross sections drop several orders of magnitude below the cross sections from electron loss.

DESIGN OF THE SIS100 CRYOCATCHER

Since the ion catchers will be located in the superconducting quadrupole doublet, their design has to account for a cryogenic environment. The cryogenic surfaces around the catcher act as a powerful cryo pump, quickly removing desorbed gases. In order to avoid condensation of gases on the surface of ion impact, the catcher will be operated at a higher temperature ($> 30\,\mathrm{K}$). Thereby, its molecular surface occupancy and the desorption yield are supposed to be low. The design of the cryocatcher including its surrounding chamber is sketched in figure 4.

As in SIS18, the ion catcher will be made of copper, coated with gold and a nickel diffusion barrier, which provides a low desorbing surface [3]. For the prototype, two different geometries are foreseen to be tested: A block catcher as indicated in figure 4, similar to the established ion catchers installed in SIS18, and a wedge catcher with a stair like structure. This catcher provides a perpendicular surface for incident ions and, in conjunction with the secondary chamber plates, it shields the circulating beam from the desorbed molecules. The distance of the ion catcher from the beam axis (35 mm) is chosen such that the accelerator acceptance is not defined by the catchers, while the catching efficiency is still high.

Cold copper plates, forming a secondary chamber around the catcher, reduce the vacuum conductance to the beam axis for the desorbed gases, and provide an additional cold pumping surface. In order to reduce the residual gas density rise during ion bombardment on the ion catcher, the aperture of the vacuum chamber around the catcher is increased relative to the beam pipe of the magnets. The wall of the secondary chamber, the distance of the front side of the cryocatcher from the chamber wall, and the increased beam aperture were optimized by means of Molflow [4] with regard to minimization of the pressure rise on the beam axis.

The outer surface of the chamber is coated with copper to provide a uniform low temperature distribution. Together with the inner secondary chamber walls, a big pumping surface emerges. The chamber coating is connected via flexible copper straps to the liquid helium return line.
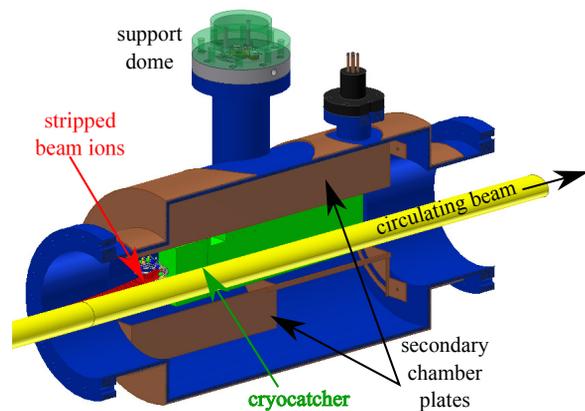
The ion catcher is thermally and mechanically hooked up in a dome. The dome is connected to the shield cooling of the cryostat. In this way, the ion catcher's temperature is stabilized to the shield temperature (50-80 K) via the thermal connection. Beam power deposited by lost ions is dissipated into the shield cooling instead of the magnet cooling circuit. Since the thermal shield and the cold chamber are now directly connected, a thermal resistance formed by the dome is necessary. Made from stainless steel, like the rest of the vacuum chamber, its thermal conductivity at cryogenic temperatures is sufficiently low. Its length and the cutaway of copper around the dome were optimized to keep the thermal load on the 5 K level acceptably small, without losing to much cold pumping surface.

In SIS100, the cryocatcher will be installed in the middle of the quadrupole doublet, inside the quadrupole-cryostat. Ten catchers per arc (60 in total) are foreseen. The vacuum chamber of the cryocatcher will also be used to evacuate the beam pipe before cooling-down. Thereby, the initial areal density of frozen gases on the cryocatcher has been minimized. The UHV-pumping port will be installed in the rear part of the vacuum chamber, where the secondary chamber surrounding the catcher is interrupted.

MACHINE PROTECTION

The cryocatcher acts as a passive and active machine protection device. The operation with intermediate charge state high intensity heavy ion beams is stabilized by minimizing the pressure rise due to ionization loss. Thereby, the build up of self-amplifying ionization losses are prevented. Additionally, the surrounding super conducting magnets are prevented from direct ion impact. The cry-
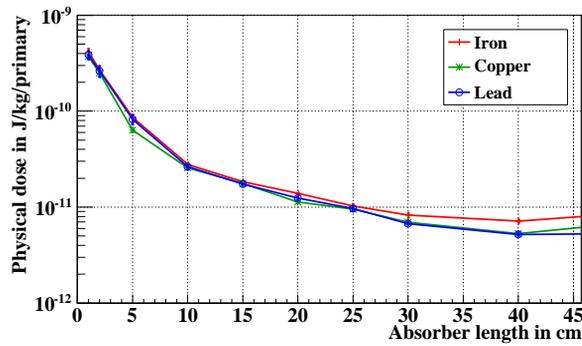
Figure 5: Average physical dose deposited in a test block behind the ion catcher for 2.7 GeV Uranium ions as a function of different catcher lengths and materials, simulated with FLUKA [5, 6].

Figure 6: Planed test-setup: Yellow: Test-beam, violett: cryocatcher, red: thermal copper-shield, gray: cryostat.

ocatcher length was thus chosen to be 25 cm such that the energy deposition in the downstream magnet is minimized, see figure 5.

The thermal design keeps the dynamic heat load onto the LHe-System low and the beam induced heat deposition is removed by the thermal shield cooling.

Since the front part of the cryocatcher will be mounted electrically insulated, the ion current and thereby the ionization losses can be measured directly. With increasing catcher current, an interlock will be triggered, protecting the machine from increasing ionization losses and heat deposition in the cryogenic system.

Additionally, the cryocatcher system defines the momentum acceptance. Ions not caught in the Rf-buckets are lost controlled and measurable on cryocatchers at the beginning of the acceleration ramp. In case of Rf-failures the catcher current will be used to trigger the emergency dumping of the beam.

SIS18-TEST OF THE PROTOTYPE CRYOCATCHER

In order to test the cryocatcher prototype under realistic condition, the installation inside a test cryostat with thermal shield and a LHe-pipe is planned (see figure 6). As foreseen in SIS100, the cryocatcher chamber will be cooled passively. The whole setup will be installed in an experimental cave at GSI and connected to the warm beam line via a cold warm transition.

Heavy ion beams from SIS18 will be used to expose the setup to realistic conditions. Different than in SIS100, the prototype cryocatcher will be irradiated directly by the primary beam. Since the SIS18 extraction energy is equal to the SIS100 injection energy, the test beam will have the same energy as the ionized beam ions hitting the cryocatcher during the SIS100 injection plateau. The currently available intensities of U^{28+} beams in SIS18 correspond to the expected loss rate in SIS100. To test the cryocatcher at higher energies, U^{73+} will be used.

The pressure rise during ion-beam bombardment inside the vacuum chamber will be measured. Different parameters, like the ion catcher temperature and its coverage by residual gas molecules, as well as the beam intensity and energy, and the ion species will be varied. The results are important input parameters for the simulation of ionization loss and dynamic vacuum effects in SIS100 with StrahlSim [7, 8].
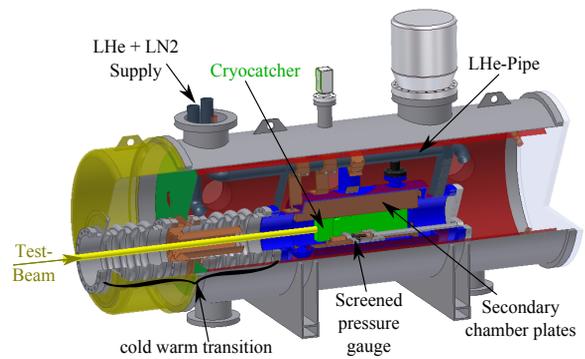
The measurement of a pressure rise in the cryogenic environment at a residual gas pressure in the order of 10^{-12} mbar requires the usage of a hot cathode extractor gauge. In order to keep the thermal radiation onto the cold surfaces low, the gauge must be screened by copper plates at 80 K. By mounting the gauge onto a pipe sticking into the prototype vacuum chamber, a placement as close as possible to the area of desorption is assured.

The construction and test of the cryocatcher prototype at GSI is a workpackage of the EU-FP7 project COLMAT. The tendering process for construction and manufacturing has been finished and the construction phase has been started. The test setup is expected to be completed at the end of 2010. A beamtime request has already been submitted and approved.

REFERENCES

[1] P. Spiller et al., Proc. of ICFA04 (2005)

[2] C. Omet, Dissertation, TU Darmstadt, Germany (2009).

[3] M. Bender, Dissertation, Goethe-Universität Frankfurt, Germany (2008)

[4] R.Kersevan, Molflow User's Guide

[5] G. Battistoni, et al., "The FLUKA code: Description and benchmarking" Proc. of Hadronic Shower Simulation Workshop 2006

[6] A. Fasso et al., "FLUKA: a multi-particle transport code" CERN-2005-10 (2005), INFN/TC_05/11, SLAC-R-773

[7] C. Omet et al., New Journal of Physics 8, 284 (2006)

[8] P. Puppel et al., Proc. of IPAC10 (2010)